Doubly Salient Permanent-Magnet Machine With Skewed Rotor and Six-State Commutating Mode

Yongbin Li[1,2] and Chunting Chris Mi[1]

[1]Department of Electrical and Computer Engineering, University of Michigan-Dearborn, Dearborn, MI 48128 USA
[2]School of Electrical Engineering, Shandong University, Ji'nan, Shandong, China

We propose new concepts for the design, optimization, and control of a doubly salient permanent-magnet machine (DSPM). We employ a uniform pole width so that the width of the rotor pole is the same as that of the stator salient pole. This design aims to minimize the cogging torque. Second, we used a skewed rotor with one-half the pole width to improve the commutation. Finally, based on the flux linkage of the skewed rotor, we used a six-state commutating mode to control the motor. We validated the feasibility of these new design concepts by simulations, field analysis, and experimental measurements of the prototype.

***Index Terms*—Cogging torque, commutating mode, doubly salient permanent-magnet machine (DSPM), pole width, skewed rotor.**

I. Introduction

THE DOUBLY SALIENT permanent-magnet machine (DSPM), a new kind of inverter-fed electrical traction motor first proposed in the early 1990s [1], is becoming more and more attractive because of its distinct features, such as high efficiency, high power density, and simple structure. Much progress has been made on the design of DSPM. For example, Liao discussed the basic principle of DSPM in 1992, 1993, and 1995, respectively [1]–[3]. Cheng and Chau studied the steady-state characteristics and performance of DSPM using nonlinear varying-network magnetic circuit analysis [4]–[8].

DSPM resembles the structure of a switched reluctance machine (SRM) except that permanent magnets are inserted in the stator. Therefore, some common techniques used in SRM are also adopted in the design and control of DSPM. For example, wider rotor pole arc, advanced shut-off angle control, and lagged firing angle control can all be used in the design and control of DSPM. However, due to the existence of permanent magnets in the stator, the behavior of DSPM is different from that of SRM. Therefore, new design and control concepts need to be explored to optimize the performance of DSPM. In this paper, a novel DSPM with skewed-rotor and six-state commutating mode is investigated. Finite-element analysis (FEA), simulations, and experimental data of the prototype verified the validity of the design concepts.

II. Skewed-Rotor Design

Fig. 1 shows the typical geometry of a DSPM with 6/4 pole pair, where AX, BY, CZ and A'X', B'Y', C'Z' are the three-phase windings. It resembles the structure of a SRM, except that permanent magnets are inserted in the stator. The three-phase flux linkages are shown in Fig. 2. Because of the existence of permanent magnets in the stator, PM flux plays a major role in the winding flux linkage. Therefore, dual-polarity control can be employed, as shown in Fig. 2, to improve its power density.

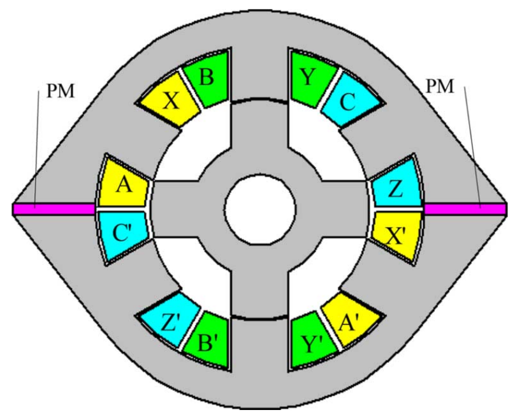

Fig. 1. Typical DSPM geometry with 6/4 pole pair.

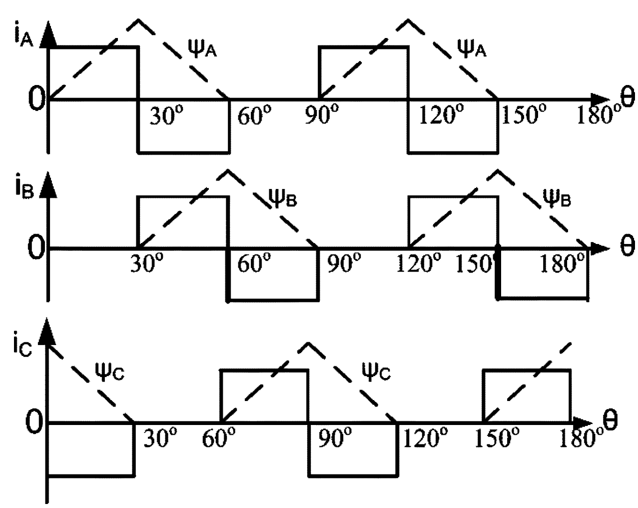

Fig. 2. Flux linkage (dashed lines) and commutating mode (solid lines).

In the design practices of SRM, in order to ensure the winding commutation and self-start capability at any rotor position and either rotating direction, there should be a small overlap between the adjacent stator and rotor salient poles when the axes of the stator pole is aligned with that of the

Digital Object Identifier 10.1109/TMAG.2007.901949

Color versions of one or more of the figures in this paper are available online at http://ieeexplore.ieee.org.

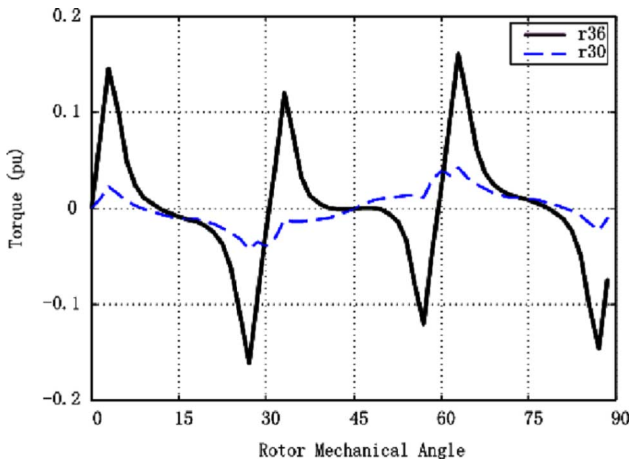

Fig. 3. Cogging torque with different rotor pole width (unskewed rotor).

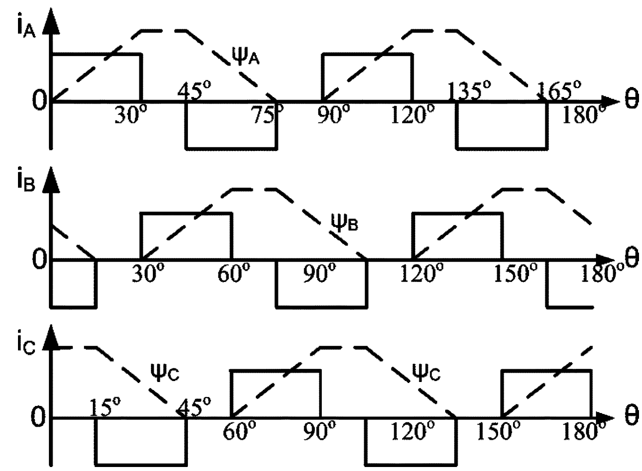

Fig. 4. Flux linkage (dashed lines) and commutating mode (solid lines) of skewed rotor DSPM.

rotor pole. Therefore, the width of the rotor pole is usually larger than that of the stator. This technology is also used in DSPM [4] because of the structure similarity. But due to the existence of permanent magnets in the stator, cogging torque exists in DSPM. According to the flux-MMF diagram of PM machines, cogging torque will reach its minimum if the resultant gap reluctance is uniform at any rotor position [9]. Therefore, for a $6/4$ pole-paired DSPM, if the width of rotor pole equals that of the stator and their width is one-half the pitch, then the cogging torque will reach its minimal value; if the rotor pole width is larger than the stator pole width, the cogging torque will increase significantly because the gap reluctance will not be uniform as the rotor position varies. Cogging torque is one of the most important issues of DSPM. The cogging torque obtained from FEA is shown in Fig. 3 for the larger rotor pole width of 36° and the uniform width of 30°. The cogging torque was calculated using 2-D FEA. It can be seen from Fig. 3 that the cogging torque is significantly less for the smaller rotor pole width. It can also be seen that the cogging torque has different peaks. This is caused by the different linkage flux from the two permanent magnets. When the rotor poles are aligned with the stator poles that are adjacent to the magnets, there is less flux leakage. Therefore, there is more cogging torque. When the rotor poles are aligned with the stator poles that are in the middle of the two magnets, more flux leakage is seen. Therefore, there is less cogging torque.

In order to minimize the cogging torque of DSPM, the width of rotor pole is designed to be the same as that of the stator, and both equal to one-half the pole pitch

$$\theta_s = \theta_r = \frac{\pi}{N_s}. \tag{1}$$

For a $6/4$ pole-paired DSPM, it is 30° mechanical degrees.

Second, a skewed rotor is used to ensure the capability of self-starting at any rotor position and either rotating direction. From the flux linkage curve, the skewed rotor can also lead to overlap between the adjacent of stator and rotor salient poles, which provides the same effect as that of the larger rotor pole width used in SRM. In order to obtain the largest output capability,

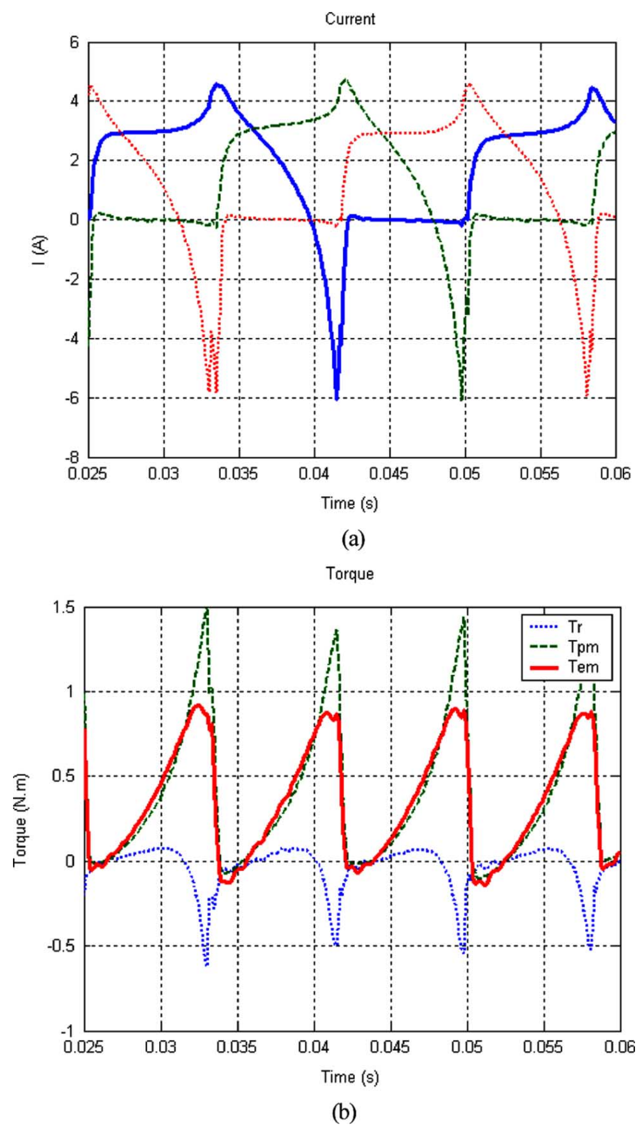

Fig. 5. Steady-state waveforms without advanced turn-off angle. (a) Three-phase current waveforms. (b) Output torque waveform.

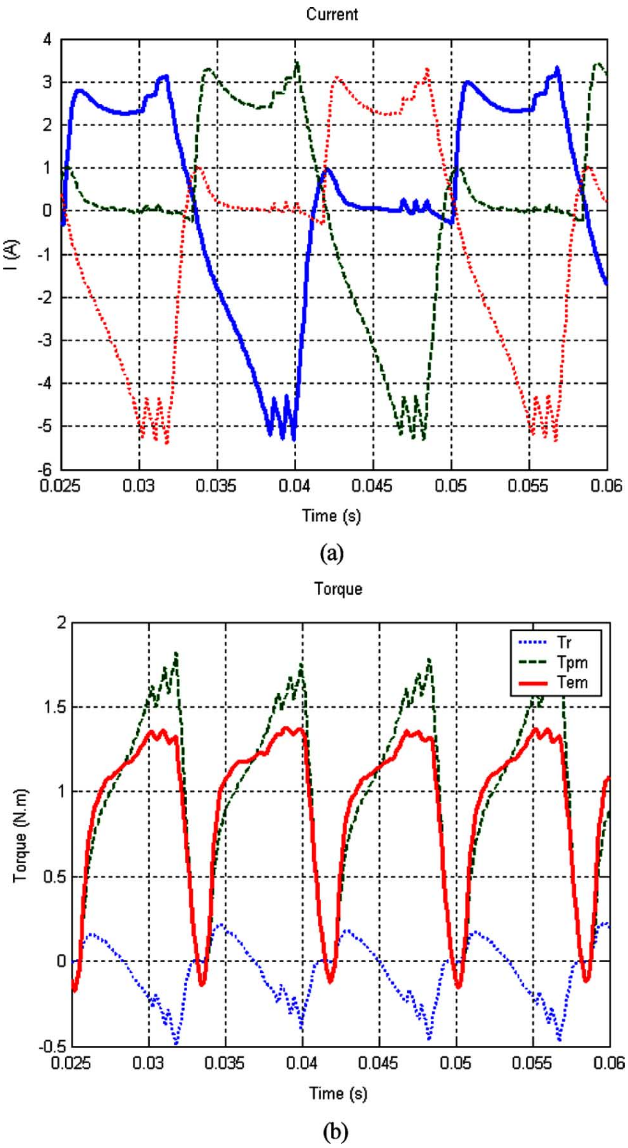

Fig. 6. Steady-state performance of DSPM with unskewed rotor. (a) Three-phase current waveforms. (b) Output torque waveforms.

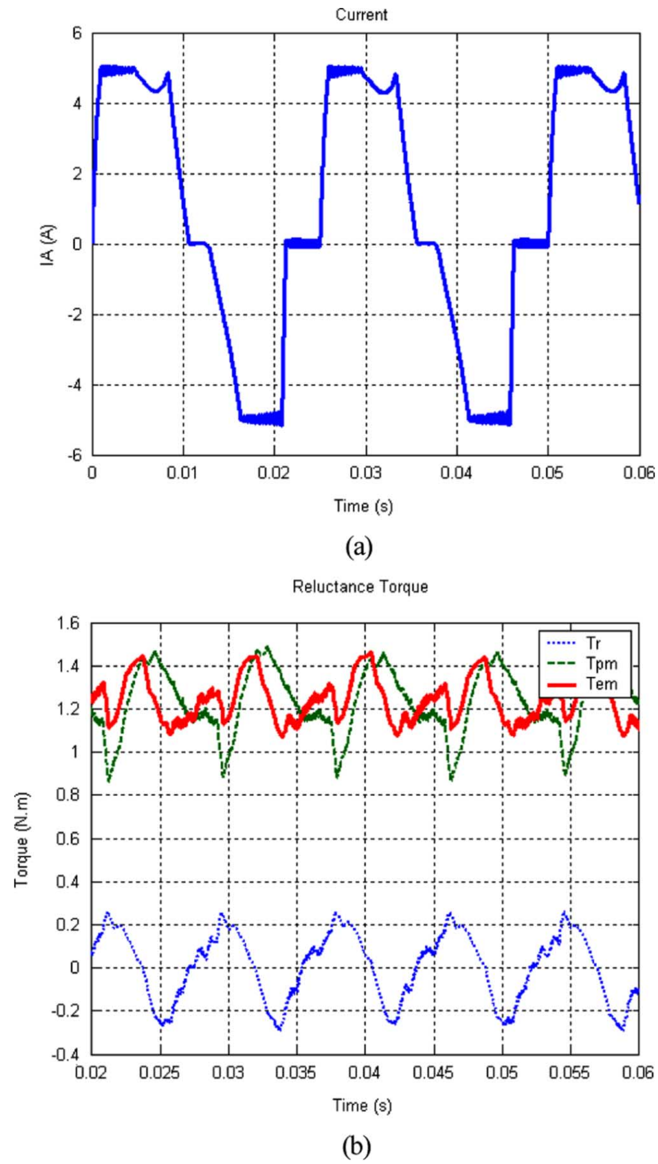

Fig. 7. Steady-state performance of DSPM with skewed rotor. (a) Three-phase current waveform. (b) Output torque waveforms.

the skew-angle is chosen to be one-half the stator salient pole width

$$\theta_{\text{skew}} = \frac{\theta_r}{2} = \frac{\pi}{2N_s}. \tag{2}$$

For a $6/4$ pole-paired DSPM, the skew-angle is 15°.

The flux linkage of the skewed rotor DSPM is shown in Fig. 4. It can be seen that the flux linkages of the skewed rotor DSPM are different from that of the unskewed rotor DSPM as shown in Fig. 2, i.e., the coverage of flux linkage is increased from 120° to 150°. As a result, the six-state commutating mode was employed.

III. Six-State Commutating Mode

In the control of conventional DSPM, three-state commutating mode was used, that is: +A-C, −A+B, and −B+C, respectively, as shown in Fig. 2. This simple commutating mode generally results in poor performance of the DSPM. It can be seen that the current commutating from positive to negative is in sequence. But in practice, because of the current continuity, the turn-off angle of the positive current should be advanced, or the freewheeling current will create a reverse torque. This will cause the control complication and decrease of output ability.

According to the same commutating principle as conventional DSPM motor, i.e., positive current conducts at the rising slope of flux linkage, while negative current conducts at the falling slope, a new commutating mode for the novel skewed rotor DSPM can be developed as shown in Fig. 4 in a solid line. It is a six-state commutating mode. The conducting sequences are +A-B, +A-C, +B-C, +B-A, +C-A, and +C-B, respectively. Each state will be conducted for 60° electrical degrees continuously, and there is a 60° interval between the positive and negative current commutation. This commutating mode makes it possible to neglect the control of turn-off angle;

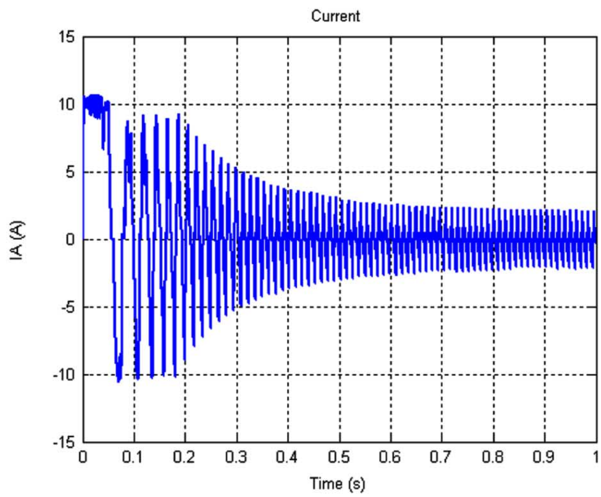

(a)

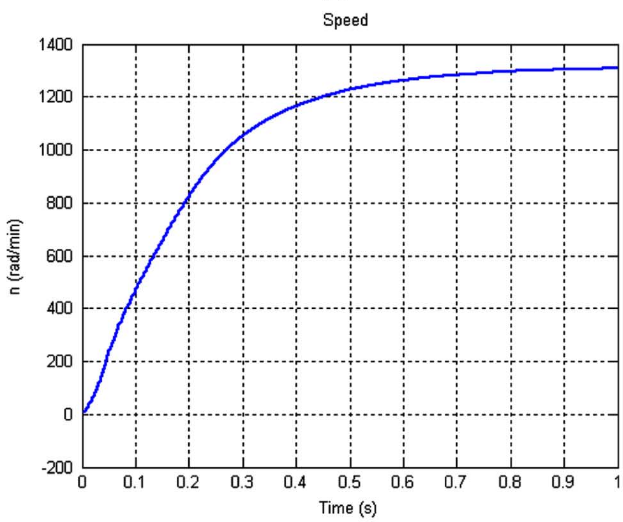

(b)

Fig. 8. Simulated starting performance of DSPM with skewed rotor. (a) Starting current waveform. (b) Starting speed waveform.

Fig. 9. Photo of the prototype rotors. Top: unskewed rotor. Bottom: skewed rotor.

therefore, commutating performance can be improved and the reliability enhanced.

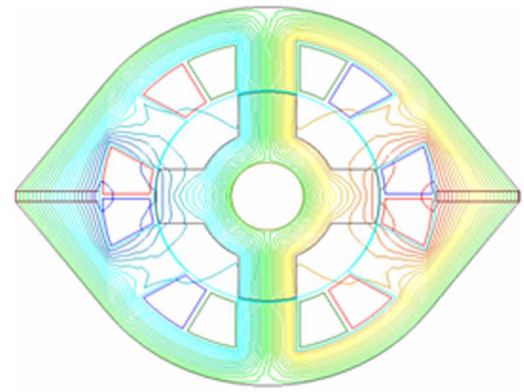

(a)

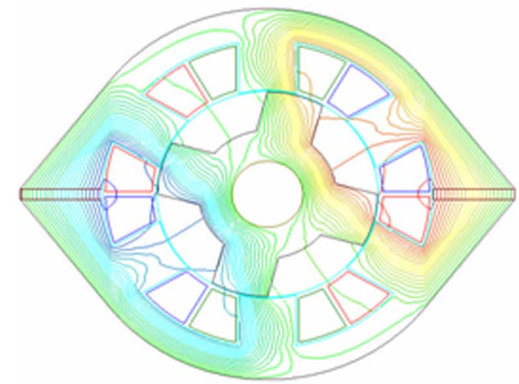

(b)

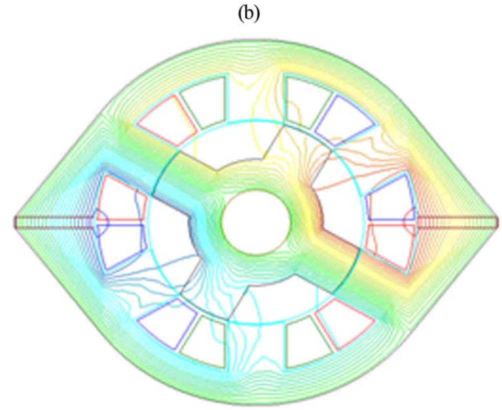

(c)

Fig. 10. Flux distributions at different rotor positions. (a) 0°. (b) 15°. (c) 30°.

IV. Simulation

In order to confirm the proposed design, the performance of the proposed DSPM is simulated. The mathematic model of DSPM can be expressed as follows:

$$\begin{cases} \dfrac{d}{dt}[\Psi] = [u] - [R]\cdot[i] \\ \dfrac{d\omega}{dt} = \dfrac{1}{J}\cdot(T_e - T_l - k_\omega\cdot\omega) \end{cases} \tag{3}$$

and

$$\begin{cases} [i] = \dfrac{1}{[L]}([\Psi] - [\Psi_{\rm PM}]) \\ T_e = \dfrac{1}{2}[i]^T\left(\dfrac{\partial}{\partial\theta}[L]\right)[i] + \left(\dfrac{\partial}{\partial\theta}[\Psi]_{\rm PM}^T\right)[i] \end{cases} \tag{4}$$

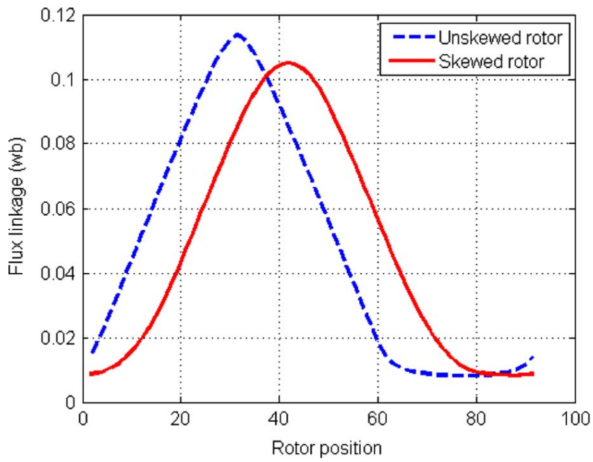

Fig. 11. Flux waveforms of the two rotor designs.

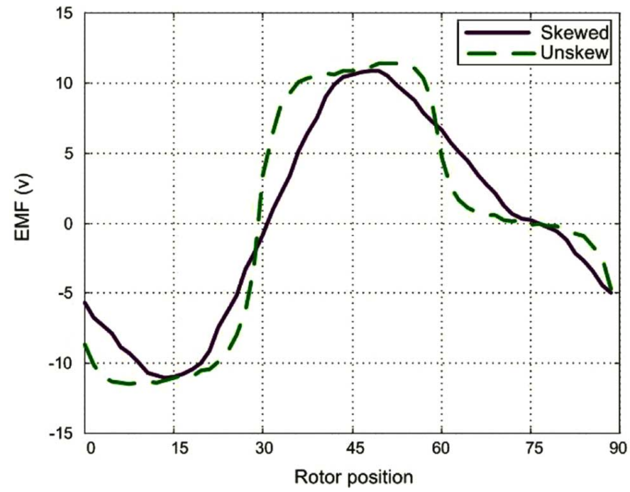

Fig. 12. EMF waveforms of the two rotor designs from FEA.

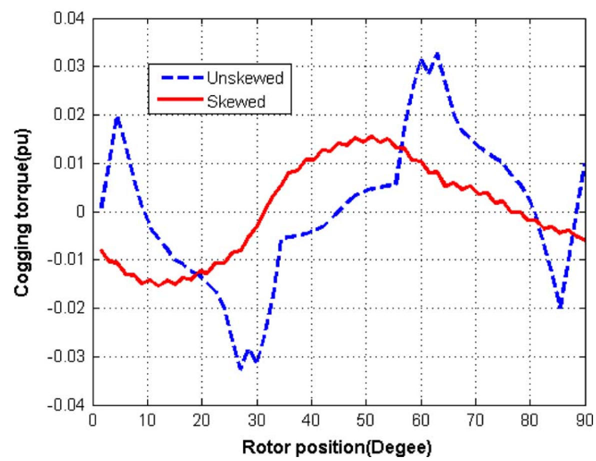

Fig. 13. Comparison of cogging torque of skewed and unskewed rotor configurations.

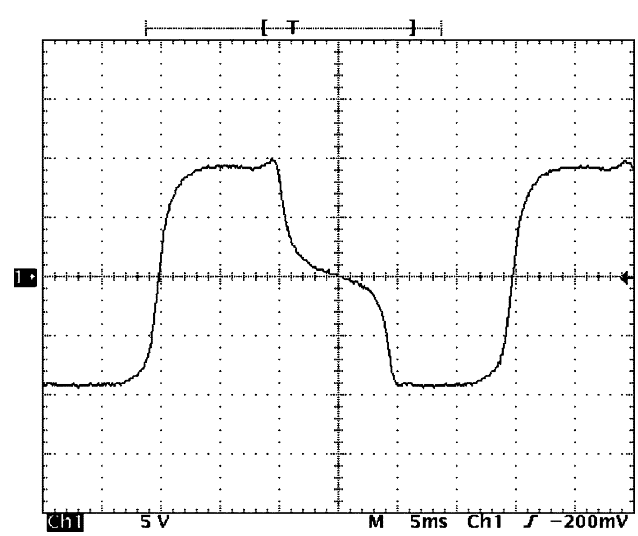

Fig. 14. Measured EMF waveform of the motor with unskewed rotor.

where $[u] = [u_A u_B u_C]^T$ is the stator voltage matrix, $[i] = [i_A i_B i_C]^T$ is the stator current matrix, $[\Psi] = [\Psi_A \Psi_B \psi_C]^T$ is the flux linkage matrix of the stator winding, $[R] = \mathrm{diag}(R_A, R_B, R_C)$ is the stator resistance matrix, $[\Psi_{\mathrm{PM}}]$ is flux linkage matrix of the permanent magnets, and $[L]$ is the stator winding inductance matrix. The PM flux and the stator winding inductance are obtained from FEA.

The simulated steady-state performances of unskewed rotor under three-state commutating mode are shown in Figs. 5 and 6, without and with advanced turn-off angle control, respectively. It can be seen from Figs. 5 and 6 that, without advanced switch-off angle control, the freewheeling current will cause asymmetrical current, which will lead to a reverse torque, fluctuant and small output torque, as shown in Fig. 5. By advancing the shut-off angle, or when the positive conducting time was shortened from 120° to 108°, the performance was improved. But the output toque ripple is still notable, and the torque also crosses over time-axis as shown in Fig. 6. Therefore, the motor cannot self-start.

The simulated steady-state performance of the skewed rotor with the six-state commutating mode is shown in Fig. 7. Compared with those shown in Fig. 6, the magnitudes of positive and negative current are more symmetrical. The output toque was increased and the torque ripple was significantly decreased. Self-start capability can be easily achieved as shown in Fig. 8.

Six-state commutating mode has been widely used in brushless DC motor (BLDC) control [10], but it was rarely discussed in the control of DSPM.

V. Prototype and Experimentation

In order to validate the proposed methods, two prototypes were designed and built: one with unskewed rotor, the other with skewed rotor as shown in Fig. 9.

The flux distributions at three different rotor positions are shown in Fig. 10. The winding flux linkages and back electromotive force (EMF) with unskewed and skewed rotor are shown in Figs. 11 and 12, respectively.

The cogging torque of the DSPM with skewed rotor was calculated using 2-D FEA by dividing the FEM model into ten slices along the axial direction, and each slice is analyzed separately. The total cogging torque is the average value of all ten slices. The simulated cogging torque of the two configurations

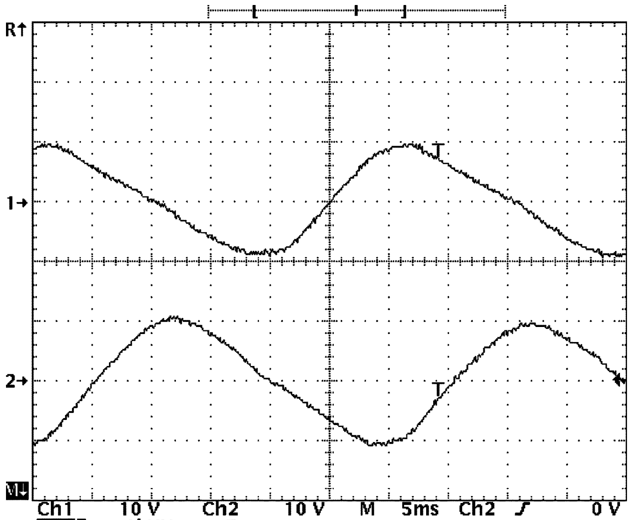

Fig. 15. Measured EMF waveforms of the motor with skewed rotor. Top curve: phase A EMF; bottom waveform, phase B EMF.

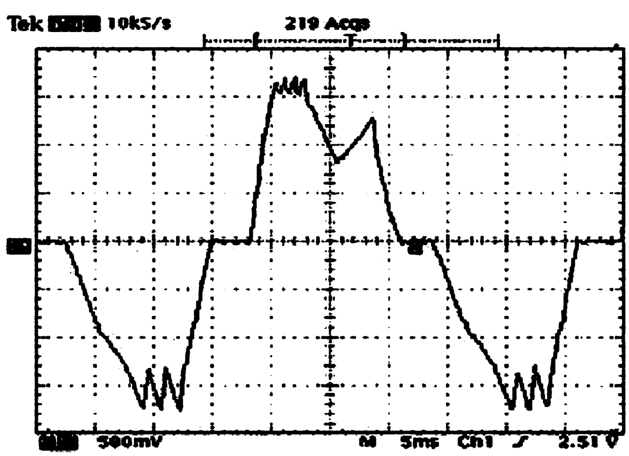

Fig. 16. Measured steady-state current waveform.

is shown in Fig. 13. It can be seen from Fig. 13 that skewing the rotor slots not only enables the self-starting capability in either direction, but also reduces the cogging torque.

A hardware control system based on ADMCF34X was developed. The measured back-EMF waveforms of the prototypes are shown in Figs. 14 and 15. The measured back-EMF coincides with the FEA results. The measured steady-state current waveform is shown in Fig. 16. The starting performance is shown in Fig. 17, which illustrated its self-starting capability. The experiment results are consistent with the simulation and FEA results.

VI. Conclusion

A new skewed-rotor design concept for $6/4$ pole-paired DSPM is proposed in this paper. In this proposed design, the rotor has the same pole width as that of the stator and skews at one-half the pole width. Based on the flux linkage of the skewed rotor, a six-state commutating mode for DSPM is presented. There are some advantages of these design concepts, such as minimum cogging torque, small torque ripple, simplified control parameters, and self-starting capability. The feasibility of these design ideas is verified by simulation and experimental results.

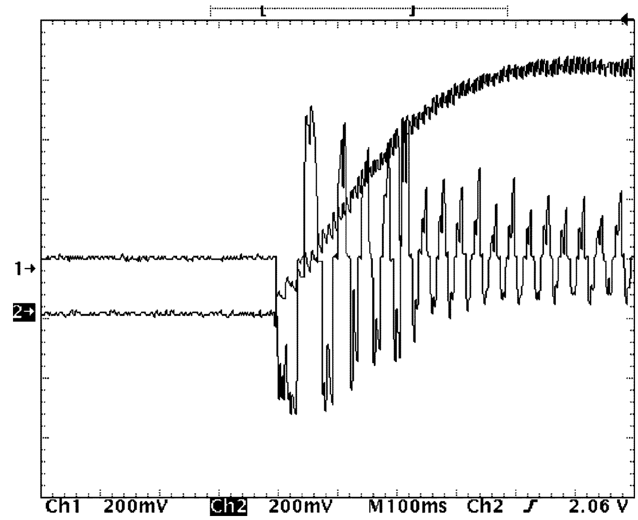

Fig. 17. Measured starting speed (trace 2) and current (trace 1) waveforms.

References

[1] Y. Liao, F. Liang, and T. A. Lipo, "A novel permanent magnet motor with doubly salient structure," in *Proc. Industry Applications Soc. Annu. Meeting*, Oct. 1992, pp. 308–314.

[2] Y. Liao and T. A. Lipo, "Sizing and optimal design of doubly salient permanent magnet motors," in *Proc. Sixth Int. Conf. Electrical Machines and Drives*, Sep. 1993, pp. 452–456.

[3] Y. Liao, F. Liang, and T. A. Lipo, "A novel permanent magnet motor with doubly salient structure," *IEEE Trans. Ind. Appl.*, vol. 31, no. 5, pp. 1069–1078, Sep./Oct. 1995.

[4] M. Cheng, K. T. Chau, and C. C. Chan, "Nonlinear varying-network magnetic circuit analysis for DSPM motors," *IEEE Trans. Magn.*, vol. 36, no. 1, pp. 339–348, Jan. 2000.

[5] M. Cheng, K. T. Chau, and C. C. Chan, "Static characteristics of a new doubly salient permanent magnet motor," *IEEE Trans. Energy Convers.*, vol. 16, no. 1, pp. 20–25, Mar. 2001.

[6] M. Cheng, K. T. Chau, C. C. Chan, and Q. Sun, "Control and operation of a new $8/6$-pole doubly salient permanent-magnet motor drive," *IEEE Trans. Ind. Appl.*, vol. 39, no. 5, pp. 1363–1371, Sep./Oct. 2003.

[7] M. Cheng, K. T. Chau, and C. C. Chan, "Design and analysis of a new doubly salient permanent magnet motor," *IEEE Trans. Magn.*, vol. 37, no. 4, pp. 3012–3020, Jul. 2001.

[8] K. T. Chau, Q. Sun, Y. Fan, and M. Cheng, "Torque ripple minimization of doubly salient permanent-magnet motors," *IEEE Trans. Energy Convers.*, vol. 20, no. 2, pp. 352–358, Jun. 2005.

[9] R. P. Deodhar, D. A. Staton, and T. J. E. Miller, "Prediction of cogging torque using the flux-MMF diagram technique," *IEEE Trans. Ind. Appl.*, vol. 32, no. 3, pp. 569–576, May/Jun. 1996.

[10] J. R. Hendershot Jr. and T. J. E. Miller, *Design of Brushless Permanent-Magnet Motors*. Oxford, U.K.: Magna Physics and Clarendon Press, 1994.

[11] Y. Li, J. Jiang, and K. T. Chau, "Research on a novel doubly-fed, doubly-salient permanent magnet machine," *CSEE*, vol. 25, no. 1, pp. 198–203, 2005.

[12] C. Martis, M. M. Radulescu, and K. Biro, "On the dynamic model of a doubly-salient permanent-magnet motor," *MELECON*, vol. 98, pp. 410–414, 1998.

[13] A. R. C. S. Babu and K. R. Rajagopal, "FE analysis of multi-phase doubly salient permanent magnet motors," *IEEE Trans. Magn.*, vol. 41, no. 10, pp. 3955–3957, Oct. 2005.

[14] Y. Fan, K. T. Chau, and M. Cheng, "A new three-phase doubly salient permanent magnet machine for wind power generation," *IEEE Trans. on Ind. Appl.*, vol. 42, no. 1, pp. 53–60, 2006.

Manuscript received February 13, 2006; revised June 5, 2007. Corresponding author: C. Mi (e-mail: chrismi@umich.edu).

Yongbin Li received the B.S.E.E. and M.S.E.E. degrees from Shandong University, Ji'nan, Shandong, China, and the Ph.D. degree from Shanghai University, Shanghai, China, all in electrical engineering.

He was an Associate Professor at Shandong University from 2000 to 2006. He was a post-doctoral researcher at the University of Michigan-Dearborn from 2006 to 2007; and before worked with University of Michigan-Dearborn, he worked as a Research Assistant at Hong Kong University in 2005. Since the beginning of 2007, he has been a Technical Specialist at Johnson Electric, Co., Hong Kong. Dr. Li has extensive research on motor design and its drives, field analysis, and MCU control. He has published more than 30 articles in these areas.

Chunting Chris Mi (S'00–A'01–M'01–SM'03) received the B.S.E.E. and M.S.E.E. degrees from Northwestern Polytechnical University, Xi'an, Shaanxi, China, and the Ph.D. degree from the University of Toronto, Toronto, ON, Canada, all in electrical engineering.

He is Associate Professor of electrical and computer engineering at the University of Michigan-Dearborn. He has conducted extensive research and published more than 60 articles on power electronics, motor drives, and hybrid electric vehicles. In addition to his position at UM-Dearborn, he is the vice chair of the IEEE Southeast Michigan section. He worked with General Electric Company from 2000 to 2001.

Dr. Mi won the National Innovation Award in 1992, the Government Special Allowance in 1994, and was listed in Marquis *Who's Who in America*. He was the winner of the 2005 Distinguished Teaching Award of the University of Michigan-Dearborn. He is a recipient of the 2007 IEEE Region 4 Outstanding Engineer Award, and the 2007 IEEE Southeastern Michigan Section Outstanding Professional Award. He recently won the 2007 SAE Environmental Excellence in Transportation (E2T) Award.